Measurement of Gas Moisture in the ppm Range Using Porous Silicon and Porous Alumina Sensors

Tarikul Islam[1**], Kalyan Kumar Mistry[2],
Kamalendu Sengupta[2] and Hiranmay Saha[1*]

[1]IC Design and Fabrication Centre, Department of Electronics and Telecommunication
Engineering Jadavpur University, Kolkata-700032
[2]Central Glass and Ceramic Research Institute, Jadavpur, Kolkata-700032

This paper reports the performance of a porous silicon (PS) sensor for detecting ppm level moisture and compares its relative performance with that of porous alumina (PA) sensors. The porous alumina sensor is fabricated by the sol-gel technique. It is found experimentally that in measuring ppm level moisture the sensitivity of the PA sensor appears to be greater than that of the PS sensor while the response time of the PS sensor is much shorter than that of the PA sensor. A simple but precise technique for the electronic measurement of sensor capacitance, which minimizes the parasitic earth capacitances, has been developed to study the response of both PS and PA gas moisture sensors. The detection electronics can be utilized for an integrated sensor unit. However, initial characterizations of both PS/PA sensors are carried out using a standard LCR meter (HP-4284A) to establish the electronic circuit.

1. Introduction

Moisture sensors must fulfill a number of requirements: they have to respond quickly, sensitively, and accurately, their temperature range should be as large as possible, and they should preferably be selective with respect to other vapours and gases. Various moisture sensors such as electrolytes, and organic polymer, ceramic and alumina thin films[1,2] have been commonly used to measure moisture content in gases at the ppm level. Although bulk sintered ceramic materials show stable physical and chemical properties, they suffer from

---

an irreversible response and a large recovery time due to chemisorption and adsorption of water molecules.[1,2] In a recent work,[3] an attempt has been made to develop a moisture sensor at the ppm level based on the capacitive technique in which the surface behavior of the alumina compacts has been taken into consideration. This sensor is sensitive to gas moisture in the range of 5–200 ppmV. However, the ceramic-based sensor poses difficulties concerning IC compatibility and fabrication. A number of studies have been reported on the development of a porous silicon (PS) relative humidity sensor because of its desirable properties such as a very large surface-to-volume ratio, controllable pore morphology and compatibility with SIC (silicon IC) technology.[4–8] A considerable number of works have been already reported concerning the development of a p-type porous silicon sensor for relative humidity sensing in order to achieve the optimized microstructure and pore morphology by controlling the electrochemical formation parameters.[7–9] However, little work has been reported on the detection of traces of gas moisture in the ppm range. Keeping in mind the well-known advantages of silicon technology, we have developed a porous silicon-based moisture sensor at the ppmV level and compare herein its performance with conventional ceramic-based ppmV level moisture sensors.

2.   Moisture Detection with Porous Silicon and Porous Alumina

The working principle of both PS- and porous alumina (PA)- based capacitive moisture sensors is that water molecules are first adsorbed from the environment into the porous layer, then the molecules diffuse into the porous sheet, stick randomly to the surface, and condense in all micropores with a radius smaller than the Kelvin radius.[5]

The condensed water vapour in the porous layer leads to a change in the dielectric constant of the porous layer, and hence the capacitance of the layer changes as a function of the moisture uptake, which is directly related to the moisture concentration in ambient gas.[8] The sensitivity, linearity and response time of these sensors are functions of the morphology and thickness of the dielectric as well as of the geometry of the contacts.[10,11] In general, the capacitance C_s of a porous silicon parallel-plate capacitor with membrane-type contact structure having two rectangular contact pads can be written as[11]

$$C_s = \frac{\varepsilon_0 \varepsilon_{sys} A}{2(t+l)} \ln\left[1 + 2\left(\frac{t+l}{d}\right)\right],$$ (1)

where $A(= b \times l)$ is the area of the each electrode, t is the total thickness of the PS and bulk silicon layers, l is the length of each electrode, d is the separation of the two electrodes, ε_0 is the dielectric constant of free space, and ε_{sys} is the dielectric constant of the system.

$$\text{If } d \gg 2(t+l), C_s \approx \frac{\varepsilon_0 \varepsilon_{eff} A}{d},$$ (2)

where ε_{eff} is the dielectric constant of the PS layer, then the PS surface capacitance predominates.

The dependency of ε_{eff} on the moisture uptake can be written as

$$\varepsilon_{eff} = f\left(\varepsilon_w \phi_w, \phi_p, T\right),$$
(3)

where ϕ_w is the volume fraction of absorbed vapour, which is related to the pore morphology of the porous layer, ϕ_p is a parameter accounting for the degree of orientation and interconnectivity of the pores, and T is the temperature in Kelvin.[6]

3. Fabrication of the Sensors

3.1 *Porous silicon*

The porous silicon moisture sensor is fabricated on an oxidized polished silicon wafer (2.5 cm × 2.5 cm × 0.5 mm) with (100) orientations having a resistivity of 1–2 Ωcm, by standard electrochemical etching in an HF-based electrolyte. A back metal contact is established by the screen-printing technique with Ag-Al paste and subsequently fired at 700°C for 45 s. The silicon wafer is then anodized in a teflon bath specially designed for this purpose, as shown in Fig. 1. The wafer actually acts as a seal between the front and back regions of the cell. The fixed front side, where the porous layer will be made, has a small circular opening of 1 cm² as shown in Fig. 1 and is exposed to a mixture of HF-CH₃OH and the rear movable side also has a similar opening exposed to a dilute KCL (5%) solution. The metal contact is in contact with the KCL solution, and is connected to the positive terminal of a power supply by graphite electrode. Another graphite electrode is used as a cathode dipped in HF solution.
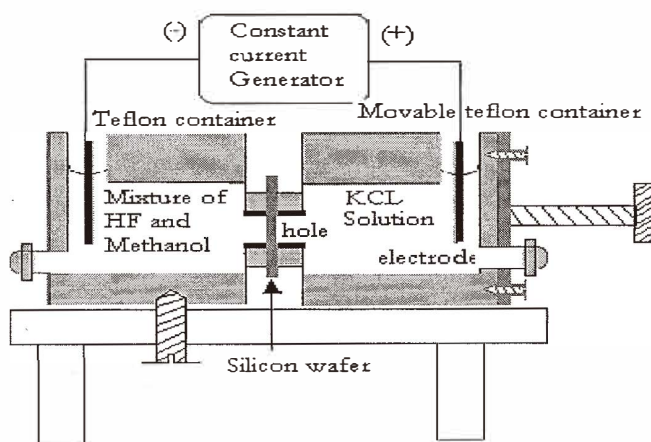

Fig. 1.   Double pond porous silicon formation bath.

The formation parameters of the sensor are a current density of 10 mA/cm^2, a HF concentration of 24% and an etching time of 5 min. Figure 2(a) shows an actual photograph of the fabricated PS sensor. The top metal contacts are developed by vacuum evaporation of aluminium. To establish ohmic contacts, the sensor is annealed in an N_2 atmosphere. Further details on the formation of the PS sensor and its performance as a function of porosity and pore morphology have been reported elsewhere.[12]

3.2 *Porous alumina*

A nanoporous alumina monolith was prepared by the sol-gel process using sec-butoxy aluminium trioxide ($C_{12}H_{27}AlO_3$) for hydrolysis and refluxing.[13] Hydrolysis was performed by mixing Al-sec-butoxide with excess water at a molar ratio of (100:1) at 90°C and stirring the mixture for 1 h on a heating bath. The suspended solution was polymerized by stirring the mixture again after adding a fixed amount of HCl (hydrochloric acid at a molar ratio of 0.07:1) at the same temperature for 1 h. A transparent sol was finally obtained by refluxing at 90–100°C for 16 h. Then, the transparent sol was dried on a flat petridish and a 70–100-μm-thick film of AlOH was formed. The film was cut into rectangles about 10 mm × 8 mm in size or circles with a radius of 12 mm and then fired to cure the film at 500°C for 10 h. After curing, the product was γ-alumina (γ-Al$_2$O$_3$) having a pore size of approximately 20 nm. Figure 2(b) shows an actual photograph of the fabricated PA sensor. The contact electrodes were printed on both surfaces of the porous alumina using Ag-Pd conducting paste to form a mesh structure. This mesh structure allows moisture to enter the pores freely. The porous alumina with two electrodes on both sides of the sample formed a parallel plate capacitor. The silver-palladium conductive paste was prepared by mixing silver and palladium in a 4:1 ratio. The mixture was ground for 5–6 h and homogenized with an organic vehicle and thinner. The organic vehicle consists of ethyl cellulose, terpenol, butyl carbetol acetate, surfactant and deflocculating agent. The paste so prepared was screen printed and dried in an air oven and finally cured at approximately 850°C. The thickness of the film was 40–50 μm.

(a)   (b)
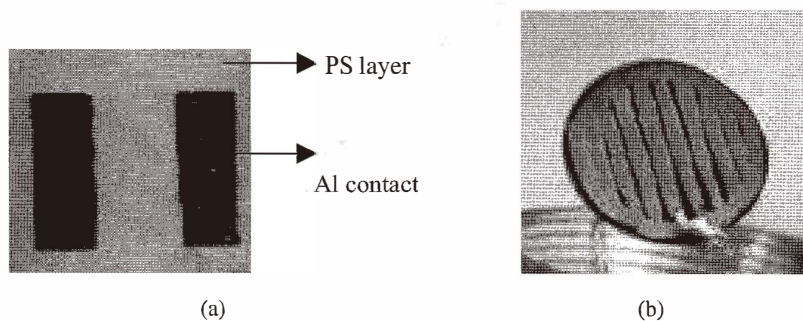
Fig. 2.   (a) Photograph of PS moisture sensor. (b)Photograph of PA moisture sensor.

4.   Detection Electronics for Sensor System

A simple circuit, which can be integrated easily with the sensor, was developed to determine the moisture-dependent capacitance. Figure 3 shows the circuit diagram of the detection electronics. It consists of an oscillator block to generate a sinusoidal input voltage, one inverting amplifier block, one rectifier circuit block, and a summing configu- ration of an opamp block. The signal frequency was chosen to be 1 kHz.[12] The output of the inverting opamp can be rectified to dc voltage using the rectifier block. In the summing block, another dc voltage with polarity opposite that of the rectifier output can be added to adjust the output of the summer by adjusting the gain of the summing amplifier. This adjustment helps to ensure that only the change in vapour concentration is measured. If one of the capacitors is a reference capacitor in a fixed environment and the other is exposed to moisture at a different concentration, then the total change in output voltage is due to moisture only. The output voltage of the inverting configuration can be given as

$$V_0 = -V_i \frac{C_2}{C_1},\tag{4}$$

where V_0 is the output of the inverting block, V_i is the input sinusoidal signal at a frequency of 1 kHz, and C_1 and C_2 are the capacitances of the two PS /PA capacitive sensors. The capacitance C_2 when exposed to water vapour can be given as

$$C_2 = \varepsilon_0 \varepsilon_{eff} \frac{A}{d},\tag{5}$$

where ε_{eff} is the effective dielectric constant of the PS capacitive sensor after exposure to moisture. Capacitance C_1 as the reference capacitance in the absence of moisture in the
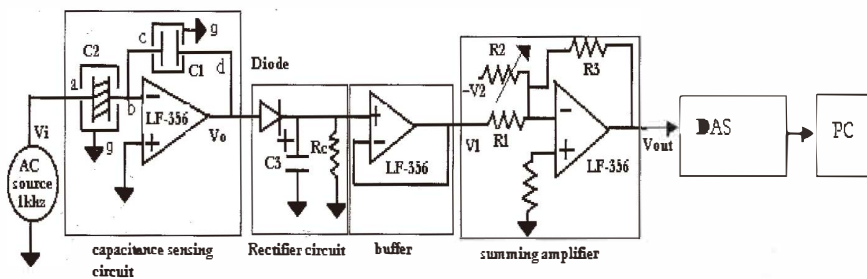

Fig. 3.   Actual capacitance measuring circuit.

feedback path of the inverting opamp can be given

$$C_1 = \varepsilon_0 \varepsilon_{ps0} \frac{A}{d},$$ (6)

where ε_{ps0} is its dielectric constant in moisture-free air. From eqs. (4), (5) and (6)

$$V_0 = -\frac{1}{\varepsilon_{ps0}} V_i \varepsilon_{eff}.$$ (7)

Because the other parameters of the PS capacitor except the dielectric constant and volume fraction of water vapour are constant, the output voltage is a function of ε_w and ϕ_w only. The output of the summing amplifier can be given as

$$V_{out} = -\frac{R_3}{R_1} V_1 + \frac{R_3}{R_2} V_2,$$ (8)

where R_3 is the feedback resistance of the summing amplifier, R_1 and R_2 are input resistances, V_1 is the output of the rectifier, and V_2 is the fixed dc voltage of opposite polarity. V_{out} can be adjusted to zero when the capacitance C_2 is at reference condition.

Generally the capacitance of a PS sensor is on the order of nF or pF, so we should consider the effect of parasitic capacitance on the precise measurement of PS capacitance. Figure 4 (a) shows the actual PS capacitor inside a grounded conducting shield, while Fig. 4(b) shows the equivalent representation of the capacitor. C_{ag} and C_{bg} are the parasitic earth capacitances of the capacitor. By having a three-terminal configuration of the capacitance, i.e., by putting the PS sensor in a conducting shield and grounding the shield, the parasitic capacitances can be made constant. As shown in Fig. 3, the terminals b and c of the capacitors C_2 and C_1 are connected to the virtual ground point of the opamp, thus
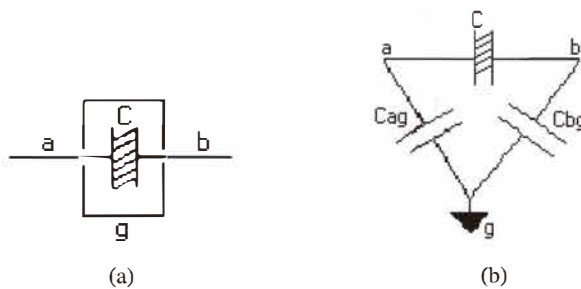

(a)   (b)

Fig. 4   (a) Three-terminal capacitance of C. (b) Equivalent circuit for C.

making the effect of parasitic capacitances C_{2bg} and C_{1cg} negligible. If the input voltage also has low internal impedance and because the stray capacitance C_{2ag} is parallel with the voltage source, its effect is smaller. Similarly, the output impedance of opamp (ideally zero) is low; the effect of C_{1dg} is smaller.[14] This circuit is thus quite insensitive to parasitic capacitance, which is an important consideration for measuring small capacitances. The complete circuit has been implemented using a low-noise low-offset high-input impedance opamp (LF-356). The output is further interfaced with a PC through a data acquisition system.

5.   Sensor Testing

The sensors were tested in an in-house designed injection test rig. The test chamber, as shown in Fig. 5, consists of a cylindrical steel case 10 cm in diameter and 12 cm high. The chamber was fitted with inlet and outlet gas pipelines. The inlet pipe was also connected to a standard thin film alumina moisture sensor to allow an equivalent amount of gas flow to the standard commercial sensor. Both PA (ceramic) and PS sensors are placed inside the chamber, and the sensors are connected with a shielded cable 2 ft long. Thus all three sensors can be exposed to equal amounts of gas flow having the same concentration of moisture. The chamber was purged with dry blended air at a flow rate of 4 litres/min. The sensors were allowed to equilibrate for several hours prior to testing. Initial measurements were taken using an LCR meter (HP 4284A). The output of the LCR meter is interfaced with a PC through a data acquisition system. The excitation voltage and signal frequency for the sensor are fixed at 1 V (rms) and 1 kHz, respectively. The following procedures were adopted. (i) Initial base line was adjusted at 6 ppmV of moisture using the standard moisture sensor. (ii) Capacitance of each sensor was noted. (iii) Test gas mixture was injected into the chamber and exposed to the sensors. (iv) Capacitance of the sensors was
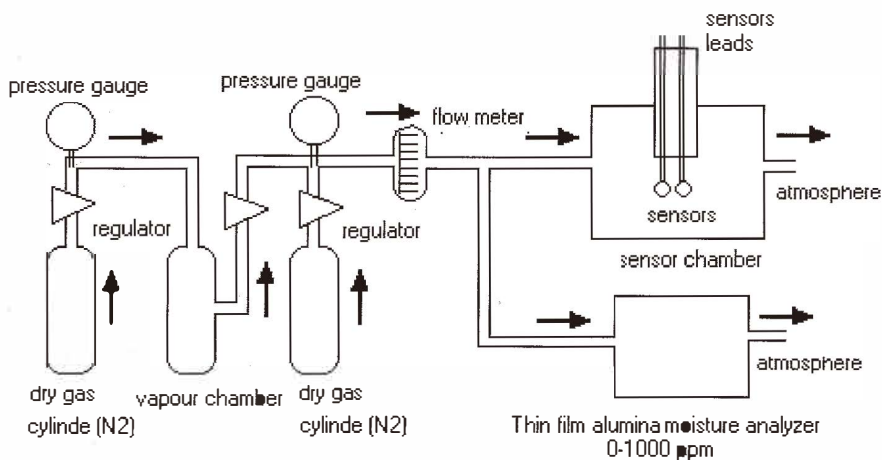

Fig. 5.   Experimental set-up for gas moisture sensor.

measured. (v) Concentration of moisture in the gas was increased from 6 ppmV to 200 ppmV and the capacitances were measured. The results of the measurements are shown in Fig. 6 and Fig. 7.

    The procedures were repeated to measure the response of each sensor using the electronic detection circuit reported earlier. Before testing, the chamber was dried with dry blended air to its previous base-line value. Results of measurements performed using the electronic circuit are shown in Fig. 8 and Fig. 9.

6. Results and Discussion

    The sensitivity of both PS and PA sensors is analyzed by putting both sensors in the measuring chamber simultaneously. The sensitivity and response time of both types of sensor are obtained under different moisture concentrations. The observations are taken by varying the moisture concentration from 5–200 ppmV. The sensitivity of the PS sensor for the change in ppmV concentration is represented graphically in Fig. 6, where the typical
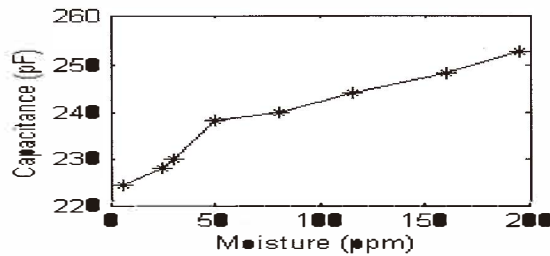

Fig. 6. Plot of capacitance change of PS sensor at different moisture concentrations of gas (ppmV) (measured by HP 4284A, 1 kHz).
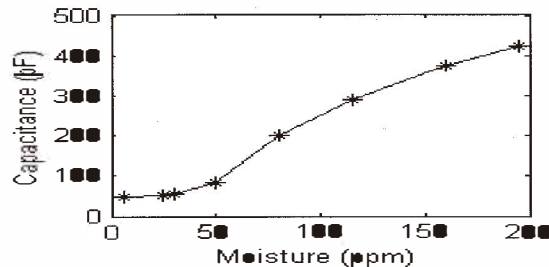

Fig. 7. Plot of capacitance change of PA sensor at different moisture concentrations of gas (ppmV) (measured by HP 4284A, 1 kHz).
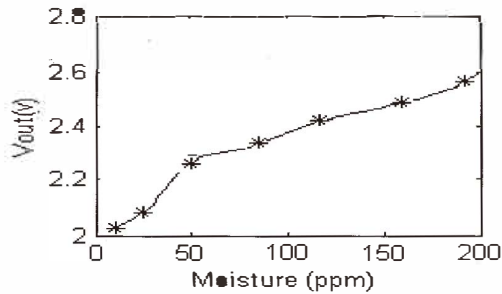
Fig. 8.   Plot of change in output voltage with ppmV moisture concentration of gas for PS sensor using electronic detection circuit.
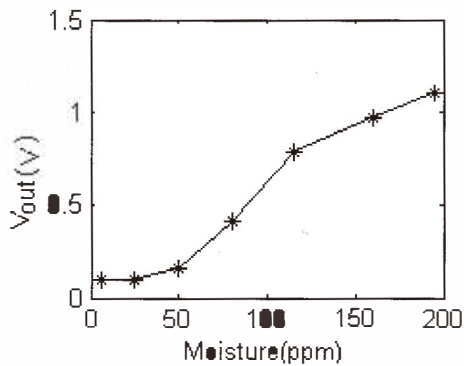

Fig. 9.   Plot of change in output voltage with ppmV moisture concentration of gas for PA sensor using electronic detection circuit.

capacitance response of the PS sensor upon exposure to ppmV level moisture present in gas is exhibited. Figure 7 represents the sensitivity of PA sensor under similar operating conditions with the same range of moisture concentrations.

It can be seen from the plot that both PS and PA sensors have good sensitivity for ppmV moisture concentrations. The variation of capacitance with gas moisture concentration is not exactly linear. The change in the absolute values of capacitance of the PA sensor is much larger than that of the PS sensor. Figures 10 and 11 show that upon exposure to moisture for a certain response time, the signal becomes stable, and after additional recovery time, the signal returns to its original value without the use of a microheater, provided no moisture covers the sensor as indicated by the standard thin film alumina moisture sensor.
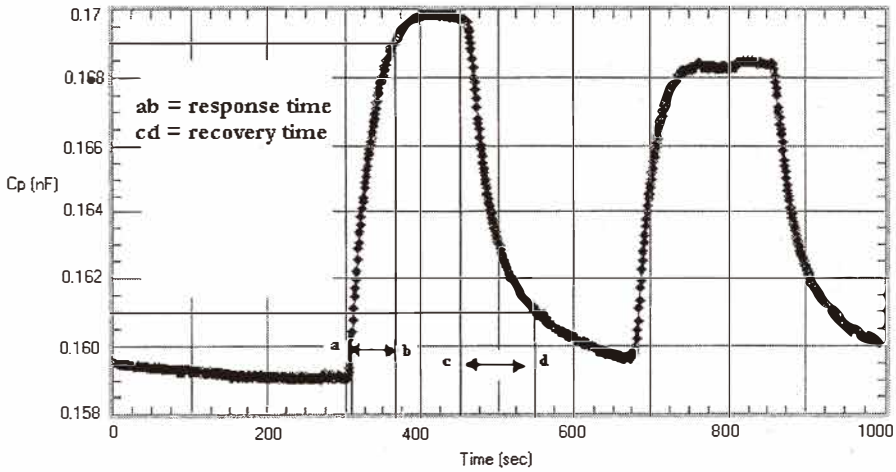
Fig. 10.   Characteristics of response and recovery of PS sensor (measured with HP 4284A, 1 kHz).
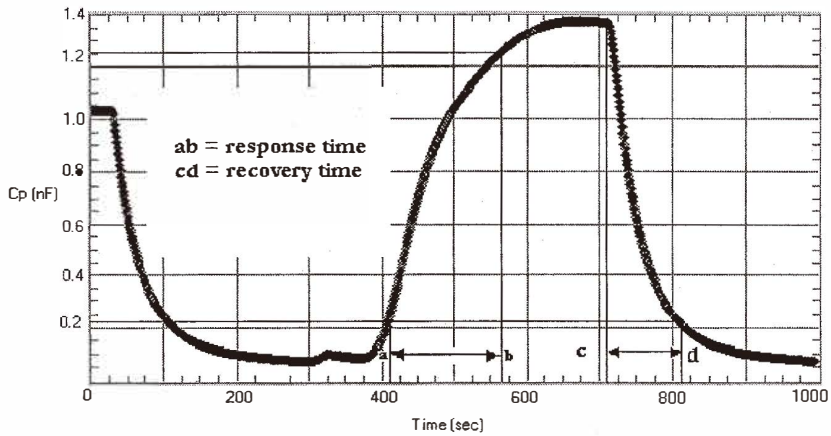

Fig. 11. Characteristics of response and recovery time for PA sensor (measured with HP 4284A, 1kHz).

    The nature of the response of both sensors is similar. The sensors react within seconds; however, it takes another few seconds to reach a stable value. Conversely, during evacuation, the water vapour concentration in the ambient decreases and the sensor reacts more slowly, however, one notices that the response of the PS sensor is much faster than that of the PA sensor. A comparison of the performance of the fabricated PS sensor with

those of a standard commercial (thin film alumina) moisture sensor and the fabricated a PA sensor is shown in Table 1. We have studied the response and recovery time of PS sensors compared to PA sensors. By applying gas with 5 ppmV–200 ppmV moisture concentration repeatedly, we observe that the PS sensor has a shorter response and recovery time than the PA sensor. This may occur because the thickness of the porous layer of the PS sensor is less than 4–5 μm, which is less than that of the PA sensor, and therefore the adsorption-desorption time is shorter. The sensitivity of the PS moisture sensor is, however, less than that of the PA sensor. It may be noted however, that neither the PS sensor nor the PA sensor has been optimized in terms of pore morphology for maximum sensitivity. The overall behavior of these two sensors may be attributed to the greater thickness and smaller dimensions of the pores of the PA layer compared with those of the PS layer. The hysteresis is a common problem in humidity sensor application based on adsorption. It is related to pore structure and pore morphology and how the presence of moisture changes this geometry. Widening the pore size in PS/PA structure or by integrating a thermoresistor in the PS/PA sensors might solve hysteresis problem slightly. Larger pores should reduce the response time but sensitivity of the sensor is also affected. There must be some hysteresis of both PS/PA moisture sensors but with present experimental facility the hysteresis analysis could not be carried out.

The output voltage of the detection electronic circuit for the same moisture concentration for the PS sensor is shown in Fig. 8. The sensitivity of the PA sensor using the detection circuit is shown in Fig. 9. We observe that the circuit suitably measures the moisture concentration of both sensors and compares favorably with the standard commercial system. The simple detection electronics can be integrated with the sensor leading to a complete ppm level moisture sensor system.

7.   Conclusion

This study investigates the suitability of a PS sensor to detect trace moisture in gases and compares its performance with that of a PA trace moisture sensor. The PS sensor is prepared by standard electrochemical etching of single-crystal silicon but the PA sensor is prepared by the sol-gel technique, a new route. The sensitivity of the PS sensor is presently

Table 1
Comparison of output responses of fabricated PS and PA sensors and standard thin film alumina moisture analyzer.

Type of sensor	Sensitivity (pF/ppmV)	Range (ppmV)	Response time (90%)	Recovery time (90%)
Fabricated PS sensor	0.25	5–200	1.2 min	1.6 min
Fabricated PA sensor	2.2	5–200	3 min	2 min
Thin film alumina sensor	500	0–200	6 min	6 min

lower than that of PA and commercially available thin film sensors, but it is sufficient to detect the trace moisture of gases. However, the response and recovery times of the PS sensor are much smaller than those of the other two types of sensors. This feature is an important consideration for developing a sensor. It is also found that for trace moisture level detection the response of the PS sensor is sufficiently linear. The sensitivity of a ppmV moisture sensor can further be improved by having an interdigital capacitance structure produced by aluminium evaporation via standard photolithography on the PS layer. A refreshing resistor around the PS layer would help desorption of water and improve the long-term stability of the PS sensor. Work is in progress to determine a suitable pore structure and pore morphology for the PS layer for increasing the sensitivity of the PS ppm level moisture sensor. To measure the capacitance of the PS and PA, a simple precise capacitance measuring circuit was designed, fabricated and tested. The circuit performs well and minimizes the parasitic earth capacitance. The design and fabrication of a PS-based sensor is simpler and economical. Above all, the PS-based sensor is IC compatible.

Acknowledgment

References

1   K. Nemoto, S. Chaturvedi, K. Hara: Technical report of I.E.I.E.C.E., OME 96–25 C.P.M. 96–38 (1996–06).
2   Z. Chen, M. -C. Jin, C. Zhen, G. -H. Chen: J.A. Ceram, Soc. **74** (1991) 1325.
3   S. Basu, M. Saha, S. Chatterjee, K. Kr. Mistry, S. Bandyopadhay and K. Sengupta: Materials Letters **49** (2001) 29.
4   O. Bisi, S. Ossicini and L. Pavesi: Surf. Sci. Rep. **38** (2000) 1.
5   J. Das, S. Dey, S.M. Hossain, Z.M. Rittersma and H. Saha: IEEE Sensors Journal. **3** (2003) 414.
6   M. J. Sailor, in L.T. Canham (Ed.): IEE Inspec, London, 1997, p.364.
7   Z. M. Rittersma and W. Benecke: Sensor and Mater. **12** (2000) 35.
8   G.M. O'Halloran: Capacitive humidity sensor based on porous silicon, Ph.D. thesis, TU Delft, (1999).
9   E. J. Connoly, G. M. O'Halloram, H. T. M. Pham, P. M. Sarro and P. J. French: Sens. Actuators A **99** (2002) 25.
10 Hcrino, G. Bomchil, K. Balra, C. Bertrand and J. L. Ginouxk: J. Electrochem. Soc. **134** (1987) 1994.
11 J. Das: Porous silicon based vapour sensing devices, Ph.D. Thesis, 2003.
12 J. Das, S.M. Hossain, S. Chakraborty and H. Saha: Sens. Actuators A **94** (2001) 44.
13 B. E. Yoldas: Journal. of Mater. Sci. **10** (1975)1856.
14 Hague, Ford: Alternating Current Bridge Method, Pitman Publishing, 1971.